Automatika

Journal for Control, Measurement, Electronics, Computing and Communications

ISSN: 0005-1144 (Print) 1848-3380 (Online) Journal homepage: https://www.tandfonline.com/loi/taut20

# An invertible dependence of the speed and time of the induction machine during no-load direct start-up

Martin P. Ćalasan

**To cite this article:** Martin P. Ćalasan (2020) An invertible dependence of the speed and time of the induction machine during no-load direct start-up, Automatika, 61:1, 141-149, DOI: 10.1080/00051144.2019.1689725

**To link to this article:** https://doi.org/10.1080/00051144.2019.1689725

AUTOMATIKA
2020, VOL. 61, NO. 1, 141–149
https://doi.org/10.1080/00051144.2019.1689725



# An invertible dependence of the speed and time of the induction machine during no-load direct start-up

Martin P. Ćalasan

Faculty of Electrical Engineering, University of Montenegro Podgorica, Montenegro

**ABSTRACT**

In this paper, an invertible dependence of the speed and time of the induction machine during no-load direct start-up is presented. Namely, based on the parameters of the induction machine equivalent circuit as well as on the basic, well-known, equation for machine torque, the analytical expression for the induction machine time-speed dependence during direct start-up is derived. On the other hand, in order to obtain inverse i.e. speed-time dependence, the derived time-speed expression is rearranged in one nonlinear equation. As the derived nonlinear equation does not have an analytical solution, a novel iterative procedure, based on the usage of Lambert W function, is proposed for its solving. The results obtained by using the developed expressions for speed-time or time-speed curves are compared with the corresponding results obtained by using expressions known in the literature as well as with the results obtained by using a numerical time-domain computation method. Moreover, the results obtained by using the developed expressions have been compared with the corresponding experimental results to demonstrate the accuracy of the derived expressions. The Matlab code developed for solving the presented iterative procedure, as well as the Matlab code for induction machine speed-time curve determination, is also provided.

**ARTICLE HISTORY**
Received 4 July 2019
Accepted 4 November 2019

**KEYWORDS**
Induction machine; mathematical modelling; starting; invertible equation

## Introduction

The Induction Machine (IM) or the asynchronous machine is a widely used electric machine in industrial and household applications. This machine has numerous advantages compared to other types of electrical machines – robustness, easy maintenance, easy control, a wide range of power/voltage, low cost, etc. [1,2]. For that reason, it has numerous applications, especially, in the industry sector and numerous directions of scientific investigation.

The IM starting process is the basic scientific and practical problem of this machine with a long tradition of observation [3–15]. The most common starting method of this machine is the direct-on-line method [3,4,8,11], which can be realized with or without the reduced voltage technique. Very popular conventional methods are also the variable rotor resistance method [9], the star-delta method [10] and the method based on the usage of auto-transformer [11–12]. The comparison between different conventional starting methods is presented in [9–11]. On the other hand, in the available literature [6,13–15] many other IM staring methods can be found. Other IM starting methods are based on the usage of soft starters [13,14] or on the shunting of the stator and rotor windings [6], whereas others require the usage of power electronic devices [15]. The comparison of conventional motor starters and modern power electronic devices for IM starting is presented in [15]. This paper deals with IM direct start-up.

The importance of an IM starting process analysis can be observed:

– from a scientific point of view and
– from an engineering point of view.

From a scientific point of view, the main direction of the IM starting process analysis is to determine the IM parameters [16–21]. There are many papers which deal with the usage of direct start-up [17,18] and with the usage of acceleration [19] and acceleration and deceleration [20,21] tests for IM parameter estimation. The general conclusion of all these methods is that the IM starting process can be very useful for parameter determination.

From an engineering point of view, the IM start-up is very important as it defines machine protection (for example, the activation of the phase current protection relay) [5,22,23] and very troublesome as it has an impact on voltage sags in local areas [11,24–27]. Namely, during the IM direct start-up, the machine current can be 6–7 times higher than the rated phase current, which can cause the activation of machine relays [12,22,23]. For that reason, the IM starting

**CONTACT** Martin P. Ćalasan martinc@ucg.ac.me Faculty of Electrical Engineering, University of Montenegro, Dzordza Vasingtona bb, 81000 Podgorica, Montenegro

process duration is very important for proper machine protection-relay settings (for example, setting of the over-current protective devices) [3–5,22,23]. In addition, the high IM phase current can cause voltage sags (for example, in distribution power systems, in small power system areas, etc.), which can have very negative implications on other loads (especially on sensitive loads such as lighting) [25–27]. Furthermore, the high value of the phase current and machine starting process duration can cause machine overheating. For that reason, many electric machine and load manufacturers provide equations for torque and power determination and their relation with starting time [28,29]. The technical description of low-voltage IMs is given in [28] and the equations, which describe three-phase IMs and proposals for the coordination of protective devices, are presented in [29]. In this paper, a mathematical modelling of an invertible dependence of the speed and time of the IM during the no-load direct start-up is presented.

The research into the IM starting time calculation is presented in several papers [3,4,28–32]. Namely, a simple mathematical equation for starting time calculation, based on machine speed, torque and mechanical parameters, is presented in [30]. However, the methods presented in technical documentation of the machine manufacturer [28,29], as well as the methods presented in [30], cannot be applied for all machines (for example, for old machines, machines without nameplate data, etc.) as they are based on manufacturer machine data.

On the other hand, the IM starting time and speed–time curves, can also be determined by using Numerical Time-Domain Computation (NTDC) methods [3,4,30]. NTDC methods assume describing the machine with a set of differential equations (differential equations for describing machine electrical circuits as well as differential equations for describing mechanical motion) and their realization or implementation in certain programme packages (for example *PSpice*, *Matlab*, *Mathematica*, etc.). However, all programme packages solve differential equations by using numerical techniques (for example – *Backward Euler method*, *Dormand–Prince method*, *Bogacki-Shampine method,* etc.) [3,4,30], and therefore require the usage of special programme packages.

Concrete research about the determination of the starting characteristics of IMs, which drive belt transport conveyers, is shown in [32]. However, the mentioned paper does not examine the IM starting speed–time characteristics at no-load conditions. Papers [3,4] also present the research about the IM starting time calculation and starting characteristics determination. More precisely, the method for starting time calculation of large IMs under conventional starting techniques (the direct start method, the star–delta method, the autotransformer method and the resistor starter method) is presented in [3]. The above paper presents the formula for IM time–speed description, which is based on the general type of mechanical load. Nevertheless, in order to prevent the infinity of the starting time and the singularity of the acceleration torque, when the formula is derived, the author proposes a certain correction factor. In addition, [3] does not deal with the inverse speed–time dependence. Finally, the mathematical modelling of IM speed–time and time–speed dependencies during no-load direct start-up is presented also in [4]. In order to obtain the relations mentioned, the machine torque is represented by using the Kloss equation. For that reason, a certain mismatching between the results obtained by using the proposed expression and experimentally determined results are noted in [4].

The goal of this paper is to determine speed–time and time–speed dependencies during no-load IM start-up, without the usage of any approximate formula (such as the Kloss equation) or any correction factors. The goal is also to compare the speed–time curve obtained by using the proposed expression with the results obtained by using expressions known from the literature (for example, as presented in [3,4]) as well as with the corresponding experimental results. Note that the invertible dependence is very important as, at any point in time, we can calculate the speed value and reversely, for any speed value we can calculate the corresponding time value.

The paper is divided into several sections. The mathematical expression for IM time–speed dependence, during no-load direct start-up, is derived and presented in Section II. Similarly, the inverse speed–time dependence, in this operating regime, is proposed in Section III. The simulation results of no-load IM direct start-up, for two IMs, based on derived expressions, as well as the results based on the expressions known in the literature and the results obtained by using a NTDC method are compared in Section IV. This section also presents certain numerical results which additionally describe the proposed speed–time expression. The comparison of experimentally determined speed–time curve during IM direct start-up and the corresponding curves determined by using the proposed expression, as well as by using expressions known from the literature are presented in Section V. The conclusions are given in Section VI – the conclusion section.

## Novel expression for time–speed curve of IM during no-load direct start-up

The mechanical equation for any rotational electrical machine is as follows:

$$J\frac{d\omega}{dt} = \sum M \tag{1}$$

where $\omega$, $J$ and $M$ represent the machine speed, the machine moment of inertia and machine torques,

respectively [4]. The previous equation can be written as follows:

$$\sum M = M_{em} - M_L - M_{loss} \tag{2}$$

where $M_{em}$, $M_L$, and $M_{loss}$ represent the machine electromagnetic torque, the torque of machine load, and the torque of machine losses (ventilation and bearings losses), respectively. By ignoring mechanical losses and observing machine start without load, (1) becomes:

$$J\frac{d\omega}{dt} = M_{em}. \tag{3}$$

The value of the machine electromagnetic torque ($M_{\text{em}}$) can be calculated by using single-cage equivalent circuit parameters as follows:

$$M_{em} = \frac{3\left(U_T/\sqrt{3}\right)^2}{\omega_s} \frac{\frac{R_2}{s}}{\left(R_T + \frac{R_2}{s}\right)^2 + (X_T + X_2)^2} \tag{4}$$

where $s$ is the machine slip, $\omega_{\text{s}}$ is the synchronous speed in [rad/s], $R_2$ is the rotor resistance referred to as the stator side and $X_2$ is the rotor reactance referred to as the stator side. On the other hand, $U_{\text{T}}$, $R_{\text{T}}$ and $X_{\text{T}}$ represent the Thevenin equivalent circuit voltage, resistance and reactance, respectively, which can be calculated as follows:

$$U_T = \frac{X_m}{X_1 + X_m} U, \tag{4a}$$

$$R_T = \frac{R_1 X_m^2}{R_1^2 + (X_1 + X_m)^2}, \tag{4b}$$

and

$$X_T = \frac{X_m R_1^2 + X_1^2 X_m + X_1 X_m^2}{R_1^2 + (X_1 + X_m)^2} \tag{4c}$$

where $X_{\text{m}}$ is the magnetizing reactance, $R_1$ is the stator resistance, $X_1$ is the stator reactance and $U$ is the supply line-to-line voltage. By using (3), IM starting time can be calculated as follows:

$$t = J \int_{\omega_0}^{\omega_f} \frac{d\omega}{M_{em}} \tag{5}$$

where $\omega_0$ is the starting speed and $\omega_f$ is the final speed [2]. Furthermore, by combining (4) and (5), and knowing that

$$s = \frac{\omega_s - \omega}{\omega_s} \tag{6}$$

we can write the following:

$$t = -\omega_s J \int_1^s \frac{ds}{\frac{U_T^2}{\omega_s} \frac{R_2/s}{(R_T + R_2/s)^2 + (X_T + X_2)^2}}. \tag{7}$$

Finally, the expression for the time–speed curve during IM direct start-up has the following form:

$$t = \frac{J\omega_s^2}{U_T^2 R_2} \cdot \left( \frac{(R_T^2 + (X_T + X_2)^2)}{2}(1 - s^2) + 2R_T R_2 (1 - s) - R_2^2 \log(s) \right) \tag{8}$$

Therefore, this expression is derived without any mathematical assumptions and without using any correction factor. However, it can be seen that this equation shows a complex relation between machine slip (speed) and time during machine direct start-up.

It should be noted that the accuracy of time–speed curve determination highly depends on the accuracy of the estimated IM parameter value. Therefore, an appropriate and accurate method for an IM parameter estimation is required. Except for acceleration and deceleration tests for an IM parameter estimation [16–21], the literature offers other very accurate methods: methods based on the measurements of different electrical variables during load operation or at standstill [33,34], a method based on observing torque–speed characteristics [35], a method based on transient analysis of IM [36], a method based on the usage of the manufacturer's data [37], etc.

## An invertible dependence for speed–time curve of IM during no-load direct start-up

By using certain mathematical modification the previously derived expression for time–speed curve (8) can be rewritten in the following form

$$\alpha + \beta \cdot e^{-\theta} = \theta \cdot e^{\theta}, \tag{9}$$

where

$$\alpha = \frac{2R_T \cdot R_2}{R_2^2} e^{\frac{J \cdot \omega_s^2 \cdot \left( \frac{R_T^2 + (X_T + X_2)^2}{2} + 2R_T \cdot R_2 \right) - t \cdot R_2 \cdot U_T^2}{J \cdot \omega_s^2 \cdot R_2^2}} \tag{10}$$

and

$$\beta = \frac{R_T^2 + (X_T + X_2)^2}{2R_2^2} e^{\frac{2 \cdot \left( J \cdot \omega_s^2 \cdot \left( \frac{R_T^2 + (X_T + X_2)^2}{2} + \cdot 2 \cdot R_T \cdot R_2 \right) - t \cdot R_2 \cdot U_T^2 \right)}{J \cdot \omega_s^2 \cdot R_2^2}} \tag{11}$$

and

$$\theta = \frac{J \cdot \omega_s^2 \cdot \left( \frac{R_T^2 + (X_T + X_2)^2}{2} + 2R_T \cdot R_2 \right) - t \cdot R_2 \cdot U_T^2}{J \cdot \omega_s^2 \cdot R_2^2} - \log(s). \tag{12}$$

As it can be seen, (9) is one highly nonlinear, i.e. transcendental equation which cannot be solved analytically. However, in this paper, we presented the following iterative procedure for solving (9).

The proposed iterative procedure requires solving the well-known Lambert W function, which has the following general form [38–40]

$$x = \beta e^{-x} \tag{13}$$

and whose solution is

$$x = W(\beta). \tag{14}$$

It should be noted that Lambert W function solving can be used for different methods or techniques: iteration methods [39], different programme packages with corresponding solvers [4] as well as analytical methods (the usage of the Taylor series [4,38] or the usage of Special Tran Function Theory – STFT [4,40–44]). The analytical methods for Lambert W solving are presented in Appendix 1.

The iteration process begins with the initial value of ${}^{(1)}\theta$ (*it can be chosen as* ${}^{(1)}\theta = 0$). After that, we need to calculate the value of the equation

$$\gamma = \alpha + \beta \cdot e^{-{}^{(1)}\theta}, \tag{15}$$

and to solve equation

$$\gamma = {}^{(2)}\theta \cdot e^{{}^{(2)}\theta} \tag{16}$$

in order to find a novel value of $\theta$. Namely, in "second step" we can write

$${}^{(2)}\theta = W(\gamma) \tag{17}$$

If ${}^{(2)}\theta$ does not satisfy the following criterion

$$|{}^{(2)}\theta - {}^{(1)}\theta| < \varepsilon, \tag{18}$$

where $\varepsilon$ is the arbitrary small real number (for example $10^{-10}$), then a new value of ${}^{(1)}\theta$ is

$${}^{(1)}\theta = {}^{(2)}\theta \tag{19}$$

and the whole procedure is repeated. Therefore, for $n$-th iteration, we can write

$${}^{(n)}\theta = W(\alpha + \beta \cdot e^{-{}^{(n-1)}\theta}). \tag{20}$$

Finally, by using the proposed iterative procedure we can determine the value of machine slip and machine speed as follows:

$$s = e^{\frac{J \cdot \omega_s^2 \cdot \left( \frac{R_T^2 + (X_T + X_2)^2}{2} + 2R_T \cdot R_2 \right) - t \cdot R_2 \cdot U_T^2}{J \cdot \omega_s^2 \cdot R_2^2} - {}^{(n)}\theta}. \tag{21}$$

and

$$n = n_s - n_s e^{\frac{J \cdot \omega_s^2 \cdot \left( \frac{R_T^2 + (X_T + X_2)^2}{2} + 2R_T \cdot R_2 \right) - t \cdot R_2 \cdot U_T^2}{J \cdot \omega_s^2 \cdot R_2^2} - {}^{(n)}\theta}. \tag{22}$$

Therefore, in order to calculate (22) we need to use the proposed iterative procedure, i.e. to solve $\theta$ whose solution depends on machine parameters and time. *Matlab* code of the proposed iterative procedure is presented in Appendix 2, while the Matlab code for the determination of the speed–time curve is presented in Appendix 3.

## Simulation results

In this section, in order to present the simulation results and to check the accuracy of the derived equations for speed–time and time–speed representation during no-load direct start-up, we observed two IMs (see Table 1). In addition, in the Matlab/Simulink programme package, we developed a simulation model which consisted of a three-phase IM, a three-phase voltage source and a block for speed measurement (see Figure 1). Therefore, we developed an NTDC method, as the Matlab/Simulink performs numerical time–domain computations. In this paper, we used a discrete simulation with a fixed step size ($10^{-5}$) for the NTDC method.

By using the data given in Table 2, for both Machine 1 and Machine 2, and by using (8) (or (22)) and (6) we determined the speed–time curve during machine direct start-up (see Figures 2 and 3 for Machine 1 and Figures 4 and 5 for Machine 2). The same figures also

**Table 1.** Induction machines parameters for simulation testing.

| Parameters | Machine 1 | Machine 2 [4] |
|---|---|---|
| $P_n$ [kW] | 3.73 | 37.3 |
| $U_n$ [V] | 575 | 460 |
| $f$ [Hz] | 60 | 60 |
| $P$ | 2 | 2 |
| $R_1$ [Ω] | 2.053 | 0.087 |
| $R_2$ [Ω] | 1.904 | 0.228 |
| $X_1$ [Ω] | 2.545 | 0.302 |
| $X_2$ [Ω] | 2.545 | 0.302 |
| $X_m$ [Ω] | 98.77 | 13.08 |
| $J_n$ [kgm$^2$]* | 0.02 | 1.662 |

Note: *Rated value of moment of inertia.

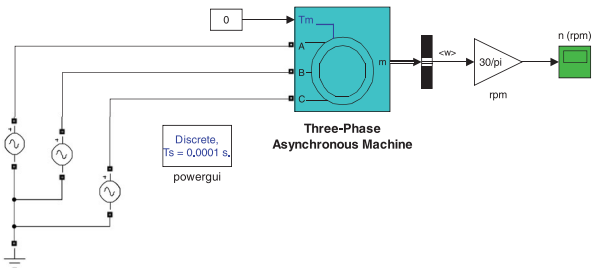


**Figure 1.** Matlab/Simulink model of IM, with three-phase supply and with block for speed measurement [4].

**Table 2.** Numerical results for the proposed iterative procedure (Machine 2).

| $t$ [s] | A | $\beta$ | k* | $\theta$ | $s$ | $n$ [rpm] |
|---|---|---|---|---|---|---|
| 0.001 | 49.4473 | $1.61 \cdot 10^4$ | 34 | 4.2186 | 0.9983 | 3.1 |
| 0.01 | 43.1972 | $1.23 \cdot 10^4$ | 33 | 4.0992 | 0.9827 | 31.1 |
| 0.1 | 11.1835 | 824.2053 | 26 | 2.9327 | 0.8168 | 329.7 |
| 0.2 | 2.4917 | 40.9131 | 18 | 1.7294 | 0.6062 | 708.8 |
| 0.3 | 0.5551 | 2.0309 | 10 | 0.7342 | 0.3654 | 1142.2 |
| 0.4 | 0.1237 | 0.1008 | 5 | 0.1749 | 0.1424 | 1543.6 |
| 0.5 | 0.0276 | 0.005 | 3 | 0.0314 | 0.0366 | 1734.1 |
| 0.6 | 0.0061 | $2.48 \cdot 10^{-4}$ | 2 | 0.0063 | 0.0084 | 1784.9 |
| 0.7 | 0.0014 | $1.23 \cdot 10^{-5}$ | 2 | 0.0014 | 0.0019 | 1796.6 |

Note: *number of iterations for error $\epsilon = 10^{-5}$.

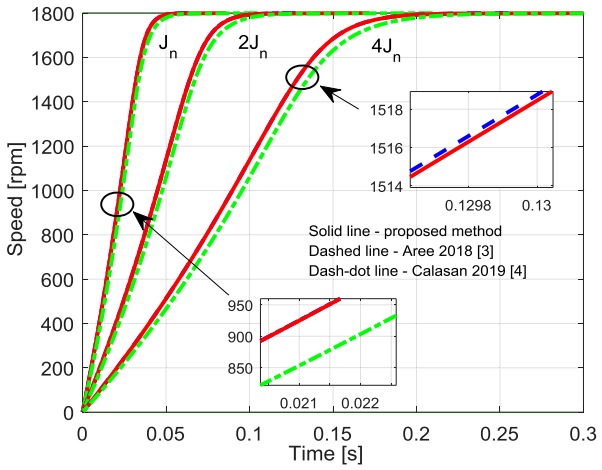


**Figure 2.** Simulation results for $U = U_n$ (Machine 1).

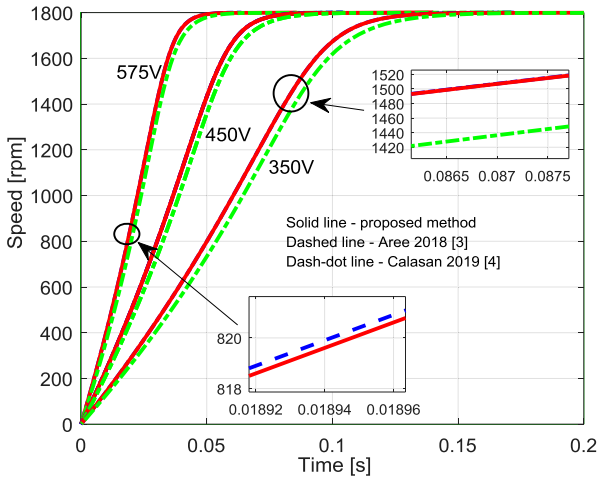


**Figure 3.** Simulation results for $J = J_n$ (Machine 1).

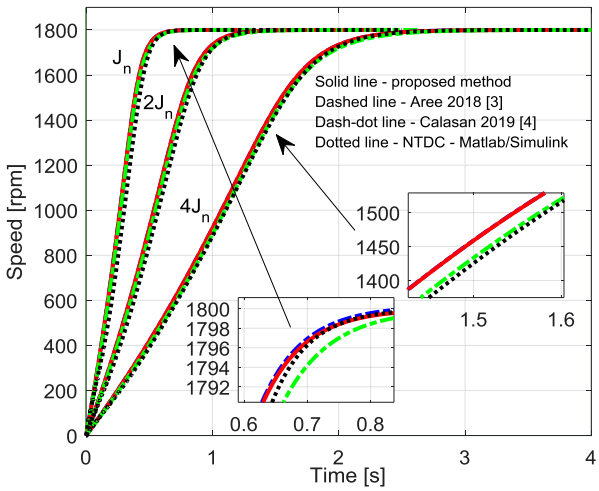


**Figure 4.** Simulation results for $U = U_n$ (Machine 2).

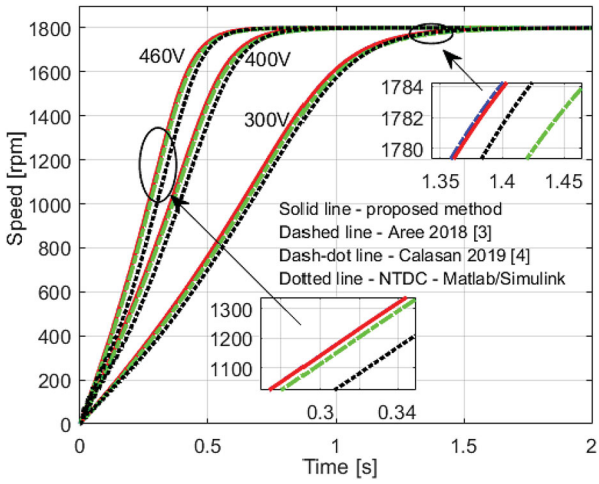


**Figure 5.** Simulation results for $J = J_n$ (Machine 2).

present speed–time dependencies obtained by using the methods (equations) proposed in [3] and [4]. The short descriptions of the methods presented in [3] and [4] are given in Appendix 4. Figures 4 and 5 also present the speed–time curves determined by using the developed NTDC method (Matlab/Simulink model – Figure 1).

For both machines, we determined speed–time dependencies for different values of supply voltage (Figures 3 and 5) as well as for different values of the machine moment of inertia (Figures 2 and 4).

As can be seen, the proposed Equation (8) or (22) enables obtaining results that are very close to the results obtained by using the method [3]. Furthermore, the speed responses obtained by using the proposed equation are found between the responses obtained by applying the methods [3] and [4] (see Figures 2–5). In addition, a good agreement between the results obtained by using the proposed method and the NTDC method is evident.

In order to show the effectiveness of the proposed iterative procedure described in Section II, some numerical results are presented in Table 2 and Table 3. As can be seen, for small values of coefficients $\alpha$ and $\beta$,

**Table 3.** Impact of calculation error on the required number of iterations (Machine 2).

| $t$ [s] | $\epsilon = 10^{-5}$ | $\epsilon = 10^{-7}$ | $\epsilon = 10^{-10}$ |
|---|---|---|---|
| 0.001 | 34 | 45 | 63 |
| 0.1 | 26 | 35 | 48 |
| 0.3 | 10 | 14 | 19 |
| 0.5 | 3 | 4 | 5 |
| 0.7 | 2 | 2 | 3 |

the speed of convergence of the proposed iterative procedure is very high (see Table 2 – only two iterations are needed) and insensitive to the initial value. In addition, if the computation error needs to be very small (smaller $\epsilon$ – see (18)), the higher number of iterations is required (see Table 3).

However, all the results obtained for two different IMs (different with respect to machine power and voltage levels) confirm the reliability and the applicability of the usage of the derived expression (8) or (22) for speed–time and time–speed curve representation during no-load direct start-up. Furthermore, as it can be seen, the presented iterative procedure (see (9)–(22)) is very efficient. It can be seen that the speed responses obtained by using the proposed method are very similar to the method described in [3]. Nevertheless, the main differences between these two methods lie in mathematical modelling. Namely, in [3] in order to prevent infinity of the starting time, during a formula derivation, the author proposes a certain correction factor, whose value need to be obtained through model testing. Also, in [3] no comments on invertible speed–time curve representation were noted. Unlike the method described in [3], the proposed method does not require the usage of any correction factor.

## Experimental results

In order to check the accuracy, applicability and simplicity of the derived Equation (8) or (22), we employed certain experimental measurement on a real set-up. The experimental set-up (see Figure 6) is composed of a three-phase IM (Leroy-Somer – 300W, 230 V, 1500r/min, 50 Hz, 1A, $\cos\varphi = 0.86$), a tachogenerator (maximum speed 10000 r/min, ratio 0.02 V/rev, together with a device for converting mechanical signals into electrical signals – MODMEC) and a variable autotransformer (maximum voltage 600 V, maximum current 10A). For current and voltage measurements, we used a power analyzer LMG as well as a MICSIG Oscilloscope.

Firstly, on this IM, we performed standard open-circuit and short-circuit tests for parameter estimation. IM single-cage equivalent circuit parameters obtained by using results from open-circuit and short-circuit tests are presented in Table 4.

Following that, we performed a direct-start-up. The direct start-up was performed at rated frequency, while

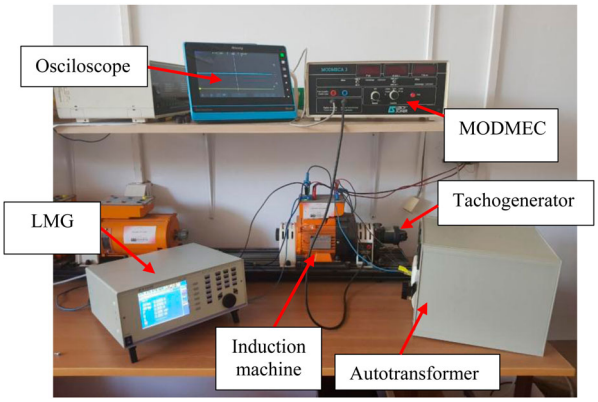


**Figure 6.** Experimental set-up.

**Table 4.** Induction machine parameters.

| Parameters | Value |
|---|---|
| $R_1$ [Ω] | 4.2 |
| $R_2$ [Ω] | 6.44 |
| $X_1$ [Ω] | 5.8 |
| $X_2$ [Ω] | 5.8 |
| $X_m$ [Ω] | 137.4 |

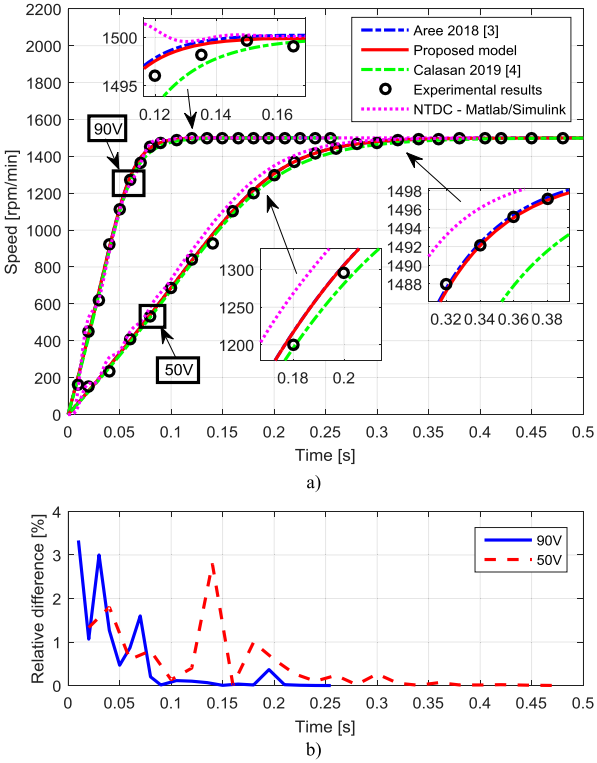


**Figure 7.** (a) Experimental and simulated results comparison, (b) Relative difference between the measured and simulated characteristics obtained by using the proposed method.

the supply voltage was 50 V, in the first experiment, and 90 V in the second experiment.

The comparison of the simulated and experimental IM speed–time curves during no-load direct start-up, for two values of supply voltage, is shown in Figure 7(a). It is evident from Figure 7(a) as well as from Figure 7(b), which represents the relative difference between the

measured and simulated speed–time curves, that the results obtained by using (8) or (22) are very close to the measured signals. Concretely, for both the simulated (obtained by using (8) or (22)) and measured signals the settling time and the rise time are almost identical. In addition, it is evident that the proposed method ((8) or (22)) better matches the experimental results than the methods presented in [4] and [3]. Furthermore, the proposed method enables obtaining results which are closer to the measured signal (see also conclusion for the results presented in Figures 2–5). At the same time, a good agreement between the results obtained by using the proposed method and the NTDC method is evident (see the zoomed part in Figure 7(a)).

Therefore, it can be concluded that the proposed Equation (8) or (22) is accurate; it is derived without any mathematical assumption and it enables obtaining results which are in very good agreement with the measured results. The derived expression can be very useful for IM protection device settings or for testing the duration of voltage sags in power networks caused by IM starting or similar.

## Conclusion

In this paper, a precise invertible dependence of the speed and time of IM during no-load direct start-up is presented. The proposed dependence is based on single-cage IM equivalent circuit parameters and the basic equation for machine torque. However, it is derived without any mathematical assumptions, as opposed to certain solutions proposed in the literature. Therefore, the presented invertible dependence for no-load direct start-up can be applied for different IMs (old, new, low or high power and voltage).

The speed–time characteristics during direct start-up for different IMs (in respect to power) obtained by using the proposed method (Equations (8) and (22)) are compared with the characteristics obtained by using expressions known from the literature. Also, a comparison between the experimentally determined and analytically determined speed–time curves (obtained by using the proposed method, as well as by using the NTDC method and literature-known methods) is also presented. All the presented results endorse the accuracy of the proposed invertible mathematical expression. Therefore, the derived speed–time dependence can be used for different engineering applications – protective device settings in power networks with an IM, settings of the IM phase current protection relay actions, testings of the impact of the IM starting process on sensitive loads, etc.

Our further research will be focused on the impact of machine losses (for example, friction losses) and different types of loads on the IM speed–time and time–speed curves during direct start-up. Also, attention will be paid to deriving mathematical expressions for speed–time and time–speed curves taking into account the machine deep-bar equivalent circuit and the machine parameter variations with slip and temperature.

## Disclosure statement

No potential conflict of interest was reported by the author.

## References

[1] Leonhard W. Control of electrical drives. 3rd ed. Berlin: Springer-Verlag; 2001.
[2] Krause PC, Wasynczuk O, Sudhoff SD. Analysis of electric machinery and drive system. New York: Wiley-IEEE Press; 2002.
[3] Aree P. Precise analytical formula for starting time calculation of medium- and high-voltage induction motors under conventional starter methods. Electr Eng Archiv fur Electron. 2018;100(2):1195–1203.
[4] Calasan M. Analytical solution for no-load induction machine speed calculation during direct start-up. Int Trans Electr Energy Syst. 2019;29(4):e2777.
[5] Bredthauer J, Struck N. Starting of large medium voltage motors: design, protection, and safety aspects. IEEE Trans Ind Appl. 1995;31(5):1167–1176.
[6] Badr MA, Abdel-Halim MA, Alolah AI. A nonconventional method for fast starting of three phase wound-rotor induction motors. IEEE Trans Energy Conv. 1996;11(4):701–707.
[7] Abdel-Halim MA, Badr MA, Alolah AI. Smooth starting of slip ring induction motors. IEEE Trans Energy Conv. 1997;12(4):317–322.
[8] Erdogan N, Henao H, Grisel R. The analysis of saturation effects on transient behavior of induction machine direct starting. IEEE Int Symp Ind Electron Ajaccio, France. 2004;2:975–979.
[9] Hamouda RM, Alolah AI, Badr MA, et al. A comparative study on the starting methods of three phase wound-rotor induction motors. I. IEEE Trans Energy Conv. 1999;14(4):918–922.
[10] Banerjee A, Banerjee A, Rana DPS, et al. A study of starting methods for an induction motor using an arbitrary waveform generator. 2015 *International Conference on Advances in Electrical Engineering (ICAEE)*; Dhaka; 2015. pp. 34–37.
[11] Goh HH, Looi MS, Kok BC. Comparison between direct-on-line, star-delta and auto-transformer induction motor starting method in terms of power quality. Int Multi Conf Eng Comput Sci Conf. 2009;II:1558–1563.
[12] Kay JA, Paes RH, Seggewiss JG, et al. Methods for the control of large medium-voltage motors: application considerations and guidelines. IEEE Trans Ind Appl. 2000;36(6):1688–1696.
[13] Solveson MG, Mirafzal B, Demerdash NAO. Soft-started induction motor modeling and heating issues for different starting profiles using a flux linkage ABC frame of reference. IEEE Trans Ind Appl. 2006;42(4):973–982.
[14] Zenginobuz G, Cadirci I, Ermis M. Performance optimization of induction motors during voltage-controlled soft starting. IEEE Trans Energy Conv. 2004;19(2):278–288.

[15] Pillary K, Nour M, Yang KH, et al. Assessment and comparison of conventional motor starters and modern power electronic drives for induction motor starting characteristics. IEEE Symp Ind Electron Appl. 2009;584–589.
[16] Pereira LA, Perin M, Pereira LFA. A new method to estimate induction machine parameters from the no-load startup transient. J Control Autom Electr Syst. 2019;30(1):41–53.
[17] Benzaquen J, Rengifo J, Albanez E, et al. Parameter estimation for deep-bar induction machines using instantaneous stator measurements from a direct startup. IEEE Trans Energy Conv. 2017;32(2):516–524.
[18] Lin WM, Su TJ, Wu RC. Parameter identification of induction machine with a starting no-load low-voltage test. IEEE Trans Ind Electr. 2012;59(1): 352–360.
[19] Jafari HK, Monjo L, Corcoles F, et al. Using the instantaneous power of a free acceleration test for squirrel cage motor parameters estimation. IEEE Trans Energy Conv. 2015;30(3):974–982.
[20] Babau R, Boldea I, Miller TJE, et al. Complete parameter identification of large induction machines from no-load acceleration deceleration tests. IEEE Trans Ind Electr. 2007;54(4):1962–1972.
[21] Despalatovic M, Jadric M, Terzic B. Identification of induction motor parameters from free acceleration and deceleration tests. Automatica (Oxf). 2005;46(3–4): 123–128.
[22] Leschert D. History of motor protection [History]. IEEE Ind Appl Magazine. 2018;24(5):6–9.
[23] Zhang P, Du Y, Habetler TG, et al. A survey of condition monitoring and protection methods for medium-voltage induction motors. IEEE Trans Ind Appl. 2011;47(1):34–46.
[24] Corcoles F, Pedra J. Algorithm for the study of voltage sags on induction machines. IEEE Trans Energy Conv. 1999;14(4):959–968.
[25] Bollen MHJ. The influence of motor reacceleration on voltage sags. IEEE Trans Ind Appl. 1995;31:667–674.
[26] Yaleinkaya G, Bollen MHJ, Crossley PA. Characterization of voltage sags in industrial distribution systems. IEEE Trans Ind Appl. 1998;34(4):682–688.
[27] Aree P. Effects of small and large induction motors on voltage sag profile. 9th International Conference on Electrical Engineering/Electronics, Computer, Telecommunications and Information Technology, Phe tchaburi; 2012. p. 1–4.
[28] ABB motor guide: basic technical information about low voltage standard motors. ISBN 952-91-0728-5; 2014. p. 52–55.
[29] ABB technical application papers, three-phase asynchronous motors: generalities and ABB proposals for the coordination of protective devices, 2009;8:30.
[30] Aree P. Starting time calculation of large induction motors using their manufacturer technical data. 19th International Conference on Electrical Machines and Systems – ICEMS; 2016. p. 1–5.
[31] Garg A, Tomar AS. Starting time calculation for induction motor. Int J Eng Res Appl. 2015;5:56–60.
[32] Popa GN, Popa I, Dinis CM, et al. Determining start time for three-phase cage induction motor that drive belt transport conveyers. 12th International Conference Optimization of Electrical and Electronic Equipment; 2010. pp. 447–452.
[33] Alturas AM, Gadoue SM, Zahawi B, et al. On the identifiability of steady-state induction machine models using external measurements. IEEE Trans Energy Conv. 2016;31:251–259.
[34] Ranta M, Hinkkanen M. Online identification of parameters defining the saturation characteristics of induction machines. IEEE Trans Ind Appl. 2013;49: 2136–2145.
[35] Monjo L, Corcoles F, Pedra J. Parameter estimation of squirrel-cage motors with parasitic torques in the torque-slip curve. IET Elect Power Appl. 2015;9:377–387.
[36] Jafari HK, Monjo L, Corcoles F, et al. Parameter estimation of wound-rotor induction motors from transient measurement. IEEE Trans Energy Conv. 2014;29:300–308.
[37] Guimaraes JMC, Bernardes JV, Hermeto AE, et al. Parameter determination of asynchronous machines from manufacturer data sheet. IEEE Trans Energy Conv. 2014;29:689–697.
[38] Corrles RM, Gonnet GH, Hare DEG, et al. On the Lambert W function. Adv Comput Math. 1996;5(1):329–359.
[39] Veberic D. Lambert W function for applications in Physics. Comput Phys Commun. 2012;183(12):2622–2628.
[40] Calasan M, Nedic A. Experimental testing and analytical solution by means of Lambert W-function of inductor air gap length. Electr Power Compon Syst. 2018;46(7):852–862.
[41] Perovich SM, Orlandic M, Calasan M. Concerning exact analytical STFT solution to some families of inverse problems in engineering material theory. Appl Math Modell. 2013;37(7):5474–5497.
[42] Perovich SM, Calasan M, Toskovic R. On the exact analytical solution of some families of equilibrium critical thickness transcendental equations. AIP Adv. 2014;4:117124–1171132.
[43] Perovich SM, Djukanovic M, Dlabac T, et al. Concerning a novel mathematical approach to the solar cell junction ideality factor estimation. Appl Math Modell. 2015;39(12):3248–3264.
[44] Perovich SM, Calasan M, Kovac D, et al. Concerning an analytical solution of some families of Kepler's transcendental equations. AIP Adv. 2016;6:035016–1-035016-23.

## Appendices

## Appendix 1

In this Appendix, two methods for solving the Lambert W equation (Equation (11)) are presented. The first method is based on the usage of the Taylor series. Namely, by using the Taylor series around 0, the solution of the Lambert W Equation (11) can be expressed as follows:

$$W(\beta) = \sum_{n=1}^{\infty} \frac{(-n)^{n-1}}{n!} \beta^n \tag{A1}$$

For practical implementation, the previous equation can be rewritten in the following form:

$$W(\beta) = \sum_{n=1}^{M} \frac{(-n)^{n-1}}{n!} \beta^n, \tag{A2}$$

where $M$ represents a positive integer. On the other hand, an asymptotic formula, which yields reasonably accurate results

for $\beta$ sufficiently large, has the following form:

$$W(B) = L_1 - L_2 + \sum_{l=0}^{\infty}\sum_{m=1}^{\infty} \frac{(-1)^l \begin{bmatrix} l+m \\ l+1 \end{bmatrix}}{m!} L_1^{-l-m} L_2^m$$
$$= L_1 - L_2 + \frac{L_2}{L_1} + \frac{L_2(-2+L_2)}{2L_1^2}$$
$$+ \frac{L_2(6-9L_2+2L_2^2)}{6L_1^3} + \ldots \quad \text{(A3)}$$

where $L_1 = \ln(\beta)$ and $L_2 = \ln(\ln(\beta))$, $\begin{bmatrix} l+m \\ l+1 \end{bmatrix}$ are non-negative Stirling numbers of the first kind [40].

Equation (11) can be also solved by using Special Trans Function Theory [40–44]. The solution of Equation (11) can be expressed in the following form:

$$x = \beta \frac{\sum_{n=0}^{M} \frac{\beta^n (M-n)^n}{n!}}{\sum_{n=0}^{M+1} \frac{\beta^n (M+1-n)^n}{n!}} \quad \text{(A4)}$$

## Appendix 2

```
% code for solving equation
% alfa+beta*exp(-theta)=theta*exp
(theta)
initial=0;
max_number_of_iteration=1000;
for current_iteration=1:max_number_
of_iteration
        current_iteration
        old_value=alfa+beta*exp
        (-initial);
        new_value=lambertw(old_value);
        if abs(new_value-initial)<
        10^-10;
        break
        end
        initial=new_value;
  end
  theta=new_value
```

## Appendix 3

```
% define value of U, J, ws, R1, R2, X1,
X2, Xm, ERROR
% determine parameters of Thevenin
circuit
UT=Xm/(X1+Xm)*U;
RT=R1*Xm^2/(R1^2+(X1+Xm)^2);
XT=(Xm*R1^2+X1^2*Xm+X1*Xm^2)/
(R1^2+(X1+Xm)^2);
% CODE
% define dt and t_final
counter=0;
for t=0:dt:t_final%dt-time step,
t_final-final speed
      counter=counter+1;
alfa=2*RT*R2/(R2^2)*exp((J*ws^2*
((RT^2+(XT+X2)^2)/2+2*RT*R2)-t*R2*
UT^2)/(J*ws^2*R2^2));
beta=(RT^2+(XT+X2)^2)/(2*R2^2)*exp
(2*(J*ws^2*((RT^2+(XT+X2)^2)/2+2*RT*
R2)-t*R2*UT^2)/(J*ws^2*R2^2));
      initial=0;
      max_number_of_iteration=1000;
for current_iteration=1:max_number_
of_iteration
current_iteration;
old_value=alfa+beta*exp(-initial);
new_value=lambertw(old_value);
if abs(new_value-initial)<ERROR;
      break
end
initial=new_value;
end
theta=new_value;
slip_value=exp((J*ws^2*((RT^2+(XT+X2)
^2)/2+2*RT*R2)-t*R2*UT^2)/(J*ws^2*
R2^2)-theta);
speed_value(counter)=(1-slip_value)
*ns;
timeaxis(counter)=t;
end
```

## Appendix 4

In [10] an analytical formula for the precise determination of IM starting time under conventional starter methods is proposed. During machine start-up, the time can be calculated as follows:

$$t = \frac{\pi J}{30} \sum_j k_j \log\left(\frac{n - n_{rj} - \zeta}{n_{lo} - n_{rj}}\right) \quad \text{(A5)}$$

where $n_{rj}$, and $k_j$ are coefficients which depend on load and machine data, while $\xi$ is the correction factor.

In [11] an analytical solution for IM speed determination during no-load direct start-up is developed. The above paper shows that the machine slip, at this operation conditions, has the following expression:

$$s = s_{br}\sqrt{W\left(\frac{1}{s_{br}^2} e^{\frac{4M_{br}}{J\omega_s s_{br}}\left(\frac{J\omega_s}{4s_{br}M_{br}} - t\right)}\right)} \quad \text{(A6)}$$

while the machine speed is

$$n = n_s\left(1 - s_{pr}\sqrt{W\left(\frac{1}{s_{br}^2} e^{\frac{4M_{br}}{J\omega_s s_{br}}\left(\frac{J\omega_s}{4s_{br}M_{br}} - t\right)}\right)}\right) \quad \text{(A7)}$$

where $M_{br}$ is the maximal machine torque and $s_{br}$ is the corresponding machine slip. On the other side, the analytical expression for IM time–speed dependence has the following expression:

$$t = \frac{J\omega_s}{2M_{br}}\left(\frac{1-s^2}{2s_{br}} - s_{br}\ln(s)\right) \quad \text{(A8)}$$